Journal of King Saud University - Science 36 (2024) 103338

HOSTED BY

Contents lists available at ScienceDirect

Journal of King Saud University - Science

journal homepage: www.sciencedirect.com

Iron oxide nanoparticles of *Cystoseira* sp. Sugar alcohol treat MRSA and thyroid gland cancer

Heba S. Abbas [a,b], Tarek A.M. Ismaeil [a], Entesar A. Ahmed [c], Doha H. Abou Baker [d,*]

[a] National Organization for Drug Control and Research recently, Egyptian Drug Authority, Giza, Egypt
[b] Microbiology Department, Faculty of Pharmacy and Drug Manufacturing, Misr University for Science and Technology, Giza, Egypt
[c] Botany and Microbiology Department, Faculty of Science (Girl Branch), Al-Azhar University, Cairo, Egypt
[d] Medicinal and Aromatic Plants Dept, Pharmaceutical and Drug Industries Institute, National Research Centre, Cairo, Egypt

ARTICLE INFO

Keywords:
MRSA
Iron oxide nanoparticles
Cystoseira sp.
Sugar alcohols
Thyroid cancer cell

ABSTRACT

Purpose: Methicillin-resistant Staphylococcus aureus (MRSA) infections are emerging as a cause of suppurative thyroiditis. The resistance to several antibiotics and finding treatment has grown more difficult. Hence, the purpose of this study was to examine biosynthesized iron oxide nanostructures' antimicrobial activity as well as their cytotoxicity on normal and thyroid cancer cells.

Methods: By using the sugar alcohols of *Cystoseira* sp., the authors synthesized the advanced biosynthesis of iron oxide nanoparticles (COINs). An agar-well diffusion method and a broth dilution method were used to investigate COINs' antimicrobial activity against MRSA isolates. However, their cytotoxicity against normal and thyroid cancer cell lines was determined by the MTT (3-(4,5-dimethylthiazol-2-yl)-2,5-diphenyltetrazolium bromide) assay.

Results: A GC–MS analysis of the dried *Cystoseira* sp. extract revealed a high percentage of D-mannitol, which is essential for the synthesis of spherical nanoparticles with a mean average size of 5.8 ± 0.8 nm. The COINs showed a higher inhibition zone (9–15 mm) for 66.6 % of MRSA isolates, and the MIC of COINs was 256 μg/ml. The cell wall of these bacteria inhabits the absorption of COINs. As a result, a large concentration of COINs is required to restrict bacterial growth. Moreover, COINs have cytotoxicity on thyroid cancer cell proliferation and normal thyroid cell lines at IC50s of 1.71 ± 0.1 and 25.9 ± 1.6 μg/ml, respectively. This can be due to the negative charge of sugar alcohols, which affect protein absorption and subsequent biological behaviors.

Conclusion: The promising findings of this study are in favor of the creation of very small iron oxide nanostructures for therapy.

1. Introduction

The thyroid gland is unusual for infections due to its massive circulatory supply, vast lymphoid drainage, high iodine levels, and anatomic encapsulation (Pearce et al., 2003). In children and young adults, up to 92 % of acute suppurative thyroiditis cases are discovered, most of which have anatomic alterations (Ghaemi et al., 2014). Acute suppurative thyroiditis symptoms comprise fever, dysphagia, and neck swelling. It foreshadowed upper respiratory illnesses (Pearce et al., 2003). Anaerobes, as well as gram-positive *Staphylococcus aureus*, are the most common pathogens (Shrestha et al., 2000). The thyroid functions are usually normal in immunocompromised patients (Pearce et al., 2003). However, thyrotoxicosis occurs when the destruction of the gland leads to the thyroid hormones' release into the bloodstream (Shrestha et al., 2000).

Infection with methicillin-resistant *S. aureus* is becoming more common. It has also been identified as a significant pathogen in the infections of head and neck. Extensive PubMed investigation revealed less than 5 published cases of Methicillin-resistant *S. aureus* (MRSA) thyroid abscess (Cabizuca et al., 2008; Elorza and Echenique-Elizonda, 2002; Lethert et al., 2006; Brook, 2009). Recently, Hadid et al. (2015) displayed that cancer patients have a high risk of MRSA and blood stream infections, which increase the rate of mortality into 35–87 % (Hadied et al., 2015; Supriya et al., 2009). MRSA infection is extremely difficult to treat because it has developed resistance to nearly all kinds of antibiotics, beginning with penicillin and, progressing to the most

* Corresponding author.
E-mail address: dohaboubaker@gmail.com (D.H. Abou Baker).

https://doi.org/10.1016/j.jksus.2024.103338
Received 9 August 2022; Received in revised form 3 July 2024; Accepted 4 July 2024
Available online 5 July 2024

Fig. 1. *Cystoseira* sp. collected from the coastal area of the Egyptian red sea.

current, linezolid and daptomycin (Kaur and Chate, 2015). As a consequence, its importance to advance novel therapeutic tactics. The fast progress of nanotechnology offers a hopeful solution to this predicament. Functional nanoformulations perform as antibacterials for MRSA infection (Gao et al., 2021).

In the future, humans will heavily rely on nanomaterials for their biomedical needs, and green nanomaterials have the advantage of being more biocompatible with human cells (Cai et al., 2008; Abbas et al., 2020; Abbas et al., 2020; Abbas and Krishnan, 2020). In the biomedical field, magnetic nanoparticles are some of the most useful metal nanoparticles (Abbas et al., 2020). Due to their magnetic properties, iron oxide nanoparticles have proven to be useful for reducing drug administration, detecting, guiding, and treating cancer Soetaert et al., 2020.

In this regard, seaweeds have also demonstrated very interesting bioactivities with their secondary metabolites, proteins, peptides, and pigments, which serve as nanofactories (Indira and Lakshmi, 2010). This is the first research to investigate the antibacterial and anticancer properties of iron oxide nanoparticles produced by the brown marine alga *Cystoseira* spp. extract against Methicillin-resistant *S. aureus* and thyroid gland cancer. *Cystoseira* spp. extract contains a variety of useful chemicals, many of which are yet unknown. The study identifies the bioactive component that has role in formation of Iron oxide nanoprticulates.

2. Methods

2.1. Materials

Cystoseira spp. were collected from the coastal area of the Red Sea, Hurghada, Egypt, during January 2019 and identified in the Faculty of Science, Al Azhar University, Cairo, Egypt. TT Cancer thyroid cell lines and Nthy-ori 3–1 normal thyroid cell lines were received from Vacsera, Cairo, Egypt. The ferric chloride anhydrous (98 %), Triton X-100, dimethyl sulfoxide (DMSO), Dulbecco's Modified Eagle Media (DMEM), p-iodonitrophenyltetrazolium violet, trifluoroacetic acid, acetonitrile, MTT salt, Muller-Hinton broth and agar (MHA), SD fine chemicals, Methicillin-resistant *S. aureus* (MRSA).

2.2. Preparation of *Cystoseira* spp. Extract

Cystoseira spp. were cleaned and kept at −20 degrees Celsius. To prepare the aqueous extract, approximately 1 g was powdered, freeze-dried, and boiled with 100 mL of distilled deionized water for 15 min in an Erlenmeyer flask with while stirring constantly. The extract was then cooled to room temperature and filtered.

2.3. Biosynthesis of iron oxide nanoparticles by *Cystoseira* spp. Extract (CIONs)

The ferric chloride salt solution 0.2 M was added to an aqueous extract of *Cystoseira* spp. in an equal volume ratio, and then the mixture was stirred for one hour and permitted to locate at room temperature for half an hour (Abbas et al., 2020).

2.4. Gas chromatography–mass spectrometry analysis (GC–MS)

The dried extract was diluted in 20 µl of pyridine and derivatized with 50 µl of N,O-bis(trimethylsilyl)-trifluoroacetamide (BSTFA) for 60 min at 70 °C. Then it was introduced into the GC/MS (Namvar et al., 2013).

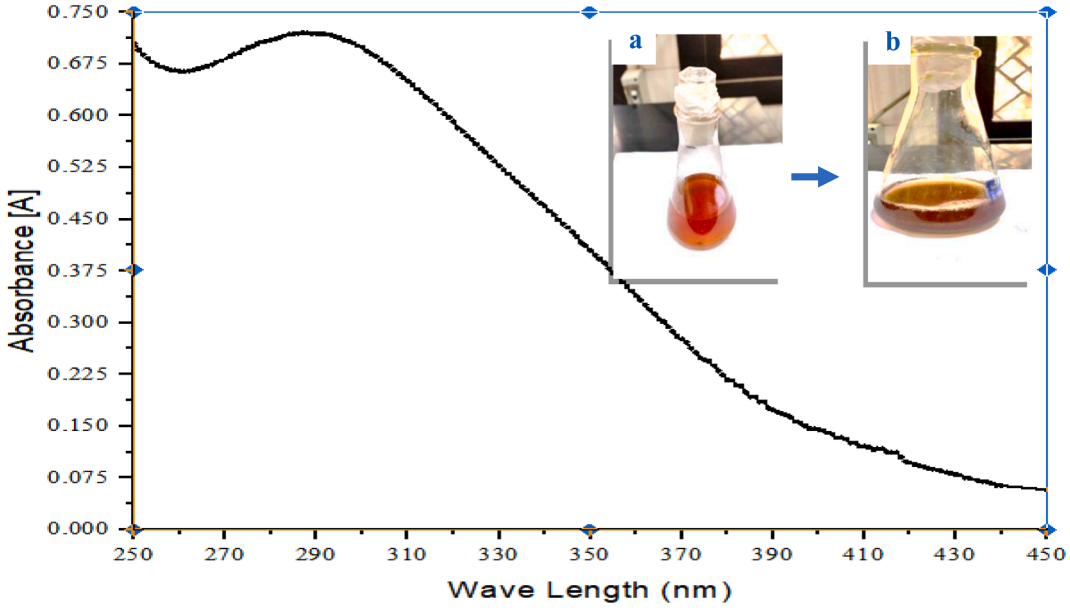

Fig. 2. UV spectrum of iron oxide Nanoparticles (black line) biosynthesized by *Cystoseira* sp. a: ferric chloride solution, and b: iron oxide nanosuspension.

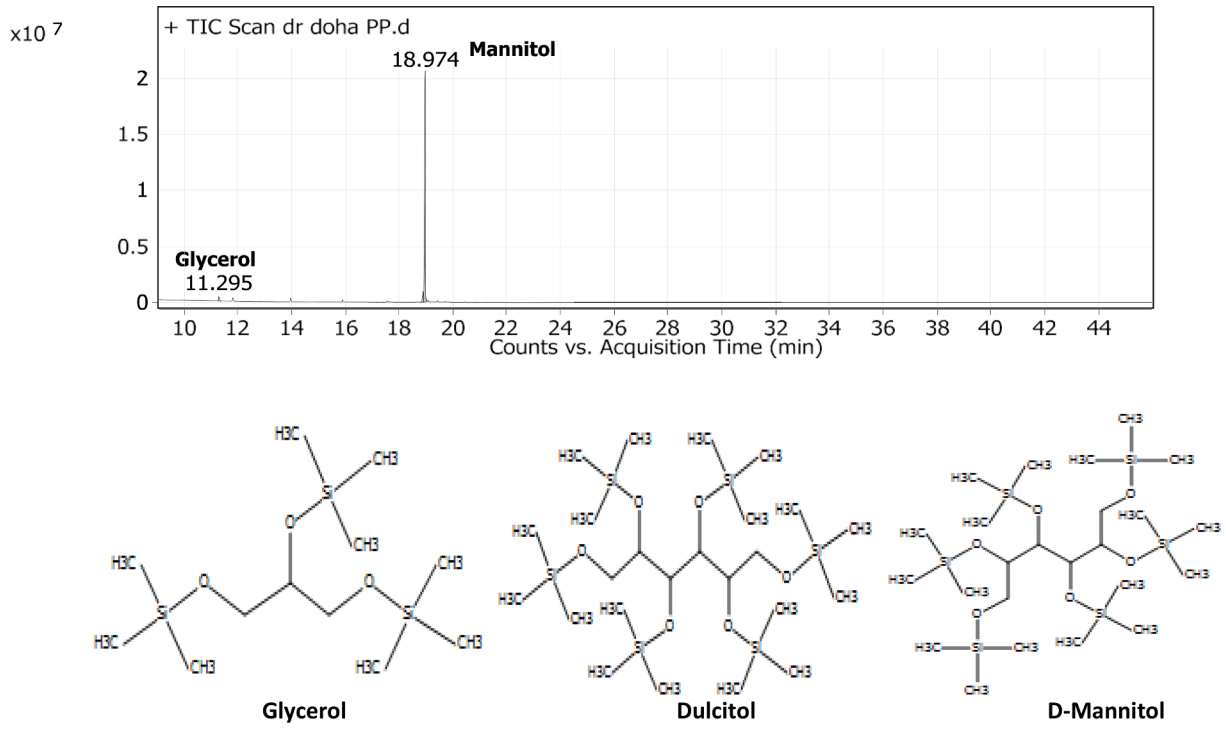

Fig. 3. GC–MS Profiling of the dried*Cystoseira* sp water extract.

Different components were identified by comparing their spectra fragmentation patterns to those recorded in Wiley and NIST Mass Spectral Library data (Namvar et al., 2013; Berkov et al., 2011).

2.5. Characterization of iron oxide nanoparticles

Biosynthesized iron oxide nanoparticles were characterized via Fourier transform infrared spectroscopy (FTIR) (JASCO 4600), Two milligrams of CIONs and algae extract were mixed with 200 mg KBr (FT-IR grade) and pressed into a pellet. Then it located into the sample holder and FT-IR spectra were recorded in the range 3500–500 cm^{-1}. Also the reduction of iron ions was measured by U-visible spectroscopy (Shimadzu UV-2600) with digital data acquisition, and wavelength range 250– 450 nm. High-Resolution Transmission Electron Microscopy (HRTEM, JEOL-JEM-2010) was used to detect the morphology, size and shape of CIONs. And the instrument was operated at an accelerating voltage of 200 kV. Drop-cast CIONs were dried under vacuum under carbon coated copper grids. Energy disperse X-ray (EDX) analysis of CIONs was carried using the same device to examine the element composition of CIONs.

2.6. Detection of Methicillin resistant s. Aureus (MRSA)

MRSA strains were received from the microbiology laboratories of Egyptian hospitals and detected in the Egyptian Drug Authority, Giza, Egypt. MRSA was detected with the use of a cefoxitin disk (30 μg) diffusion. The culture was done on a Mueller-Hinton agar plate with 0.5 McFarland standard of *S. aureus* broth. After allowing the lawn culture to dry for about 5 min, a cefoxitin disk (30 μg) was placed on top of it. Finally, the agar plate was incubated for 18 h at 35 °C. MRSA strains had a zone of inhibition diameter of less than 21 mm, whereas Methicillin-susceptible *S. aureus* strains had a zone of inhibition diameter of more than 22 mm (CLSI, 2500).

2.7. Antibiotics susceptibility test for Methicillin resistant s. Aureus (MRSA)

Antimicrobial sensitivity of nine MRSA isolates was detected by disk-diffusion method. Bacterial suspensions (0.5 McFarland tubes) of MRSA were inoculated on Mueller-Hinton agar. The antibiotic disks of 6-mm diameter were purchased from Oxoid, Basingstoke, UK; Amikacin (AMK) 30 μg; Ceftriaxone (CRO) 30 μg; Ampicillin / sulbactam (SAM) 10/10 μg; amoxicillin/clavulanic acid (AUG) 20/10 μg; Ceftazidime (CAZ)30 μg; cefoxitin (fox) 30 μg; Ciprofloxacin (CIP) 5 μg; and cefotaxime (CAZ) 30 μg; Erythromycin (E) 30 μg; Vancomycin (VA) 30 μg, and Linezolid (LAZ) 30 μg were placed on the plates and incubated at 37 °C for 24 h. The diameter of inhibitory zone was determined in millimeters according to Masood et al. (2010), and the Clinical and Laboratory Standards Institute (CLSI 2012 and 2020) (CLSI, 2500; Masood and Aslam, 2010; CLSI, 2500).

2.8. Screening for the antibacterial activity of Cystoseira sp iron oxide nanoparticles (CIONs)

The antibacterial activity of iron oxide nanoparticles was investigated against nine clinical strains of methicillin-resistant *S. aureus* by using the agar-well diffusion method. The Muller Hinton Agar (MHA) plates were inoculated with 0.5 McFarland turbidity of MRSA according to the National Committee for Laboratory Standards (CLSI) for 2020 and 2012 (CLSI, 2500; Masood and Aslam, 2010; CLSI, 2500). The antimicrobial activity was measured by measuring the inhibition zone using the Himedia Zone Reader (Thomas et al., 2012). MIC was determined as the lowest concentration of antimicrobial test substance as described previously by Balouiri et al. (2016), Makky et al.(2021) (Balouiri et al., 2016; Makky et al., 2021).

2.9. Cell viability assay

In 96-well microtiter plastic plates, we grew TT Cancer thyroid cell lines and Nthy-ori 3–1 normal thyroid cell lines for 24 h under 5 % CO2 in fresh complete growth medium. Cells were incubated either alone or

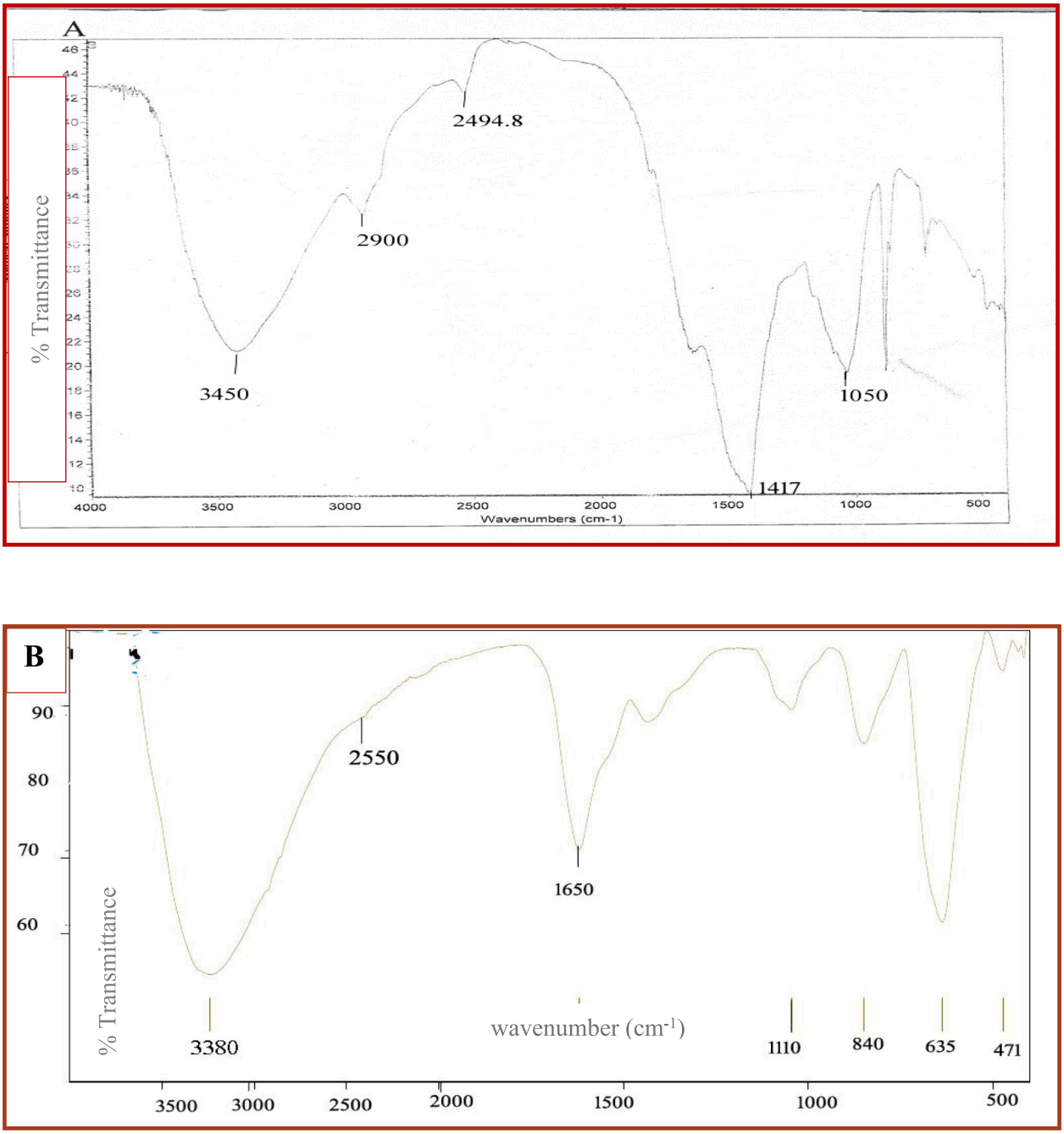

Fig. 4. FTIR of the dried*Cystoseira sp* water extract (A) and biosynthesized iron oxide Nanoparticles (B).

with iron oxide nanoparticles to give a final concentration of 0.39, 1.56, 6.25, 25, and 100 µg. After 48 h incubation, sodium dodecyl sulphate (SDS) was added to each well and incubated overnight at 37 °C to dissolve the crystals. The absorbance at 595 nm on a microplate multi-well, 620 nm was used as the reference wavelength. MTT assay were performed as described by El-Menshawi et al. (2010) (El-Menshawi et al., 2010).

3. Results

In the coastal area of the Egyptian Red Sea, Cystoseira brown algae (order Fucales, family Surgaassaceae) have distinct basal and apical regions, and have air-vesicles. (Fig. 1). Further, the main axis of *Cystoseira* spp. is elongated foliage, and their lowest sections, known as foliar expansions or basal leaves, are heavily flattened (Fig. 1). In our study, iron oxide nanoparticles (CIONs) biosynthesized by allowing *Cystoseira* spp. water extract to react with 0.2 M $FeCl_3$ solution, and the reactions took place at room temperature. Consequently, the yellowish brown ferric chloride solution became a dark brown colloidal solution. The UV spectrum of CIONs was analyzed by using a UV–visible spectrophotometer (Fig. 2).The absorbance peaks at 290 nm confirmed the formation of the monodispersed iron oxide nanoparticles.

The GC–MS profiling of the dried Cystoseira *sp.* extract showed three sugar alcohol compounds, including glycerol, dulcitol (galactitol), and D-mannitol,and the highest percentage was for D-mannitol (94.9 %) (Fig. 3). However, the percentages of glycerol and dulcitol in the extract were 1.41 % and 3.6 %, respectively.

Our intent was to identify the functional groups involved in the biosynthesis of iron oxide nanoparticles by comparing their IR spectrum with that of dried *Cystoseira* spp. (Fig. 4). The IR spectra of dried

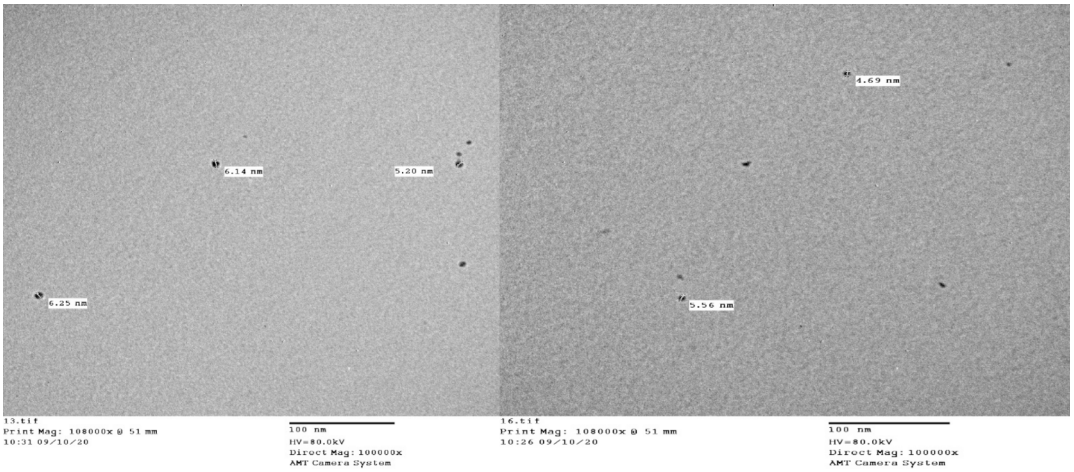

Fig. 5. HRTEM micrograph of *Cystoseira* sp. extract mediated iron oxide Nanoparticles (CIONs).

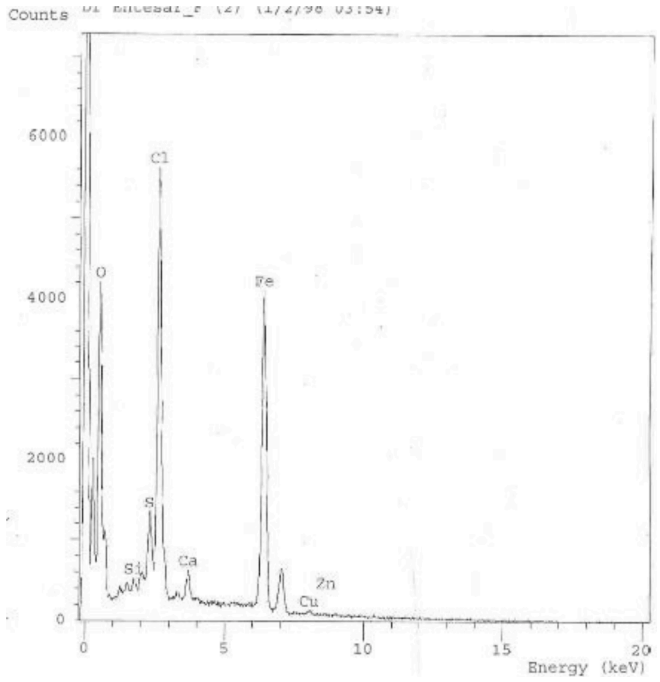

Fig. 6. Energy Disperse Xray for *Cystoseira* sp. extract mediated iron oxide Nanoparticles (CIONs).

Cystoseira spp. extract indicated several functional groups as follows: 3450 cm − 1 represents the O–H group of sugar or alcohol, while 2900 cm − 1 indicates the existence of aliphatic C–H stretching vibrations. Further, 2494.8 cm − 1 and 1417 cm − 1 showed the presence of O–H bending alcohol, whereas 1050 cm − 1 proved the presence of C-O stretching vibration of alcohol. In addition, iron oxide nanoparticles displayed an intense absorption spectra for O–H at 3.380 cm-1, and red shift were noticed for2494.8 cm − 1,1050 cm − 1of O–H bending, and C–O stretching vibration alcohol to 2550 cm–1, and 1110 cm–1, respectively. A C = C stretching vibration of conjugated alkene was also detected at 1,650 cm-1. Our findings are consistent with recent GC mass spectroscopy data that demonstrated the presence of sugar alcohol in *Cystoseira* spp. extract.

The HRTEM images of CIONs revealed monodispersed spherical forms with sizes ranging from 4.62 nm to 7.62 nm, with a mean average size of 5.8 ± 0.8 nm. (Fig. 5).

The structure of materials present in CIONs was examined using EDX. The purity level of the nanoparticles was analyzed, which confirms that Cystoseira spp. extract- mediated iron oxide Nanoparticles have 31.6 %±4.5 of iron, and 46.72 %±4.4 of oxygen, respectively (Fig. 6). The Cl signals must originate from the ferric chloride precursor used in the protocol of biosynthesis. Also, other signals by elements such as Si, Cu, Zn, and Ca originated from the algae that mediated the biosynthesis. The presence of iron and oxide peaks confirms the formation of iron oxide nanoparticles.

Table 1
Compounds identified from *Cystoseira* sp. extract.

S. N	Peak Name	Retention Time	Peak Hight	Peak area	% Area
1	Glycerol 3TMS derivatives Formula: C12H32O3Si3 Molecular weight: 308.6372	11.295	383316.08	635479.04	1.41
2	Dulcitol 6TMS derivatives Formula: C24H62O6Si6 Molecular weight: 615.2585	18.898	975608.19	1615390.68	3.6
3	D −Mannitol 6TMS Formula: C24H62O6Si6 Molecular weight: 615.3	18.974	20631583.12	42529543.33	94.9

On Mueller Hinton agar plates, an antibiogram for different Staphylococcus aureus strains was assessed using the disk-diffusion technique and interpreted according to the CLSI guidelines. On the basis of resistance to third- and second-generation antibiotics such as cefoxitin, cefotaxime, and ceftriaxone, isolates were identified as MRSA during a multidrug-resistant (MDR) investigation. To confirm the presence of MRSA, the MDR pattern of the isolates was examined with different antibiotics from the cephalosporin and methicillin groups. All Staphylococcus aureus isolates were highly susceptible to vancomycin, linezolid (100 %), amikacin (66.6 %), and erythromycin (66.6 %) (Table 1). They were highly resistant to amoxicillin + clavulanic acid (100 %), cefoxitin, ampicillin/sulbactam, ceftriaxone (100 %), erythromycin (66.6 %), and ciprofloxacin (66.6 %) (Table 1).

The antimicrobial activity of COINs nanosuspensions has been screened using the agar well diffusion technique. The COINs nanosuspensions showed higher antimicrobial activity against MRSA isolates

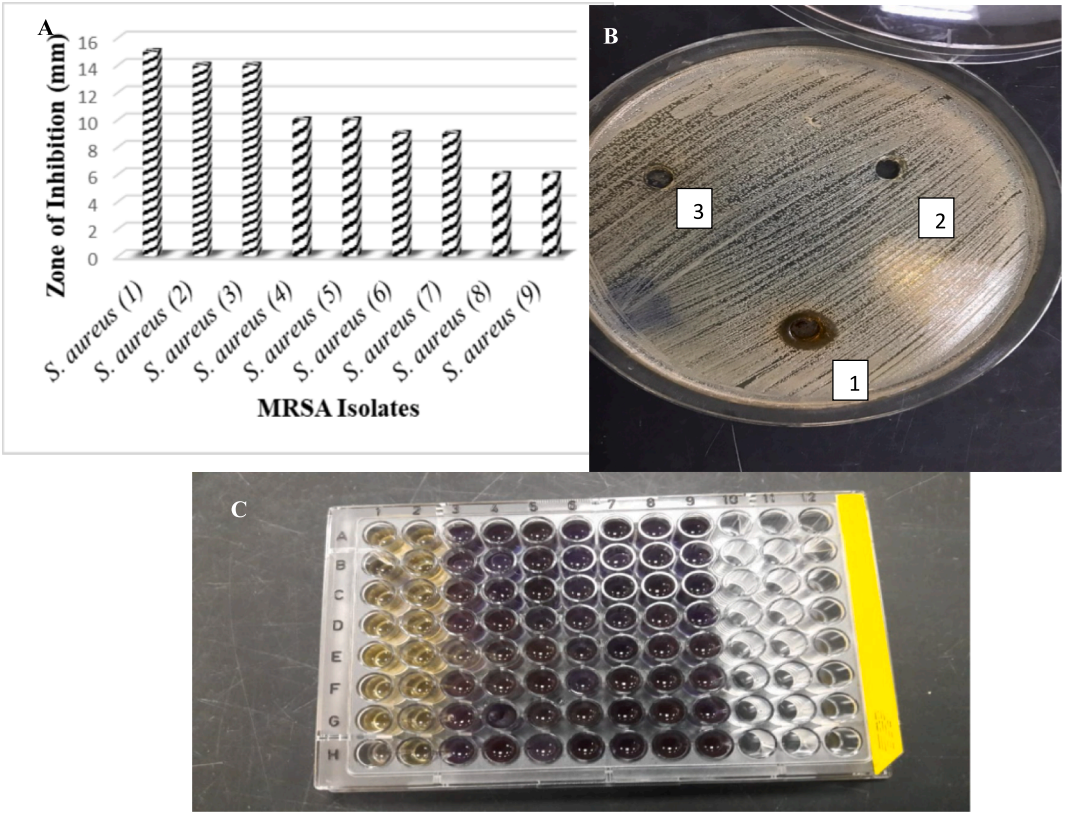

Fig. 7. Antimicrobial activities of COINS Against MRSA Isolates (a) By using agar diffusion method, (b) Against MRSA no. 4, 1: COINs, 2: DMSO, 3: Algae water extract, (c) MIC determination with INT dye; 1:8 lanes are 512 to 2 µg COINs with MRSA, and 9 lanes are MRSA isolate as negative control.

Table 2
Antibiogram for different *Staphylococcus aureus* strains by using the disk-diffusion technique.

Antibiotics	Antibiotics Family	*S. aureus* (1)	*S. aureus* (2)	*S. aureus* (3)	*S. aureus* (4)	*S. aureus* (5)	*S. aureus* (6)	*S. aureus* (7)	*S. aureus* (8)	*S. aureus* (9)
Amikacin (AMK)	Aminoglycosides	R*	S*	S	S	R	R	S	S	S
Amoxicillin + clavulanic acid (AUG)	Aminopenicillin	R	R	R	R	R	R	R	R	R
Cefoxitin (FOX)	2nd generation cephalosporin	R	R	R	R	R	R	R	R	R
Ampicillin/ sulbactam (SAM)	Aminopenicillin	R	R	R	R	R	R	R	R	R
Erythromycin (E)	Macrolides	R	S	S	R	R	R	R	R	R
Vancomycin (VA)	Glycopeptide	S	S	S	S	S	S	S	S	S
Cefotaxime (CTX)	3rd generation cephalosporin	R	R	R	R	R	R	R	R	R
Ceftriaxone (CRO)	3rd generation cephalosporin	R	R	R	R	R	R	R	R	R
Ciprofloxacin (CIP)	Fluoroquinolone	S	S	S	R	R	R	R	R	R

(*) R: resistant, and S: sensitive.

compared to DMSO alone and the aqueous Cystoseira spp. extract (Fig. 7a). The COINs nanosuspensions showed an inhibition zone (9–15 mm) for 66.6 % of MRSA isolates, as shown in Fig. 7b. However, the inhibition zones of amikacin, linezolid, vancomycin, and, in some cases, erythromycin and ciprofloxacin were higher (14–21 mm).

According to the microdilution method, the growth of MRSA was decreased when it was cultured with 128, 256, and 512 µg/ml of COINs. Visual examination of bacterial growth as turbidity or pellets in the wells of the microtiter plate to determine the minimum inhibitory concentration is difficult. Colorimetric approaches are appealing because they have the ability to produce distinct endpoints based on a visible color shift. The tetrazolium salt p-iodonitrophenyltetrazolium violet (INT) was used as a bacterial growth indicator for our study. INT is a chemical that is converted to a violet INT formazan product by bacterial dehydrogenases in metabolically active bacterial cells, as in 128 to2µg/ml of COINs concentrations and the negative control (Fig. 7c). The minimum inhibitory concentration of COINs by 100 % to 256 µg/ml for 88.8 % of MRSA isolates and to 128 µg/ml for 11.1 % of MRSA

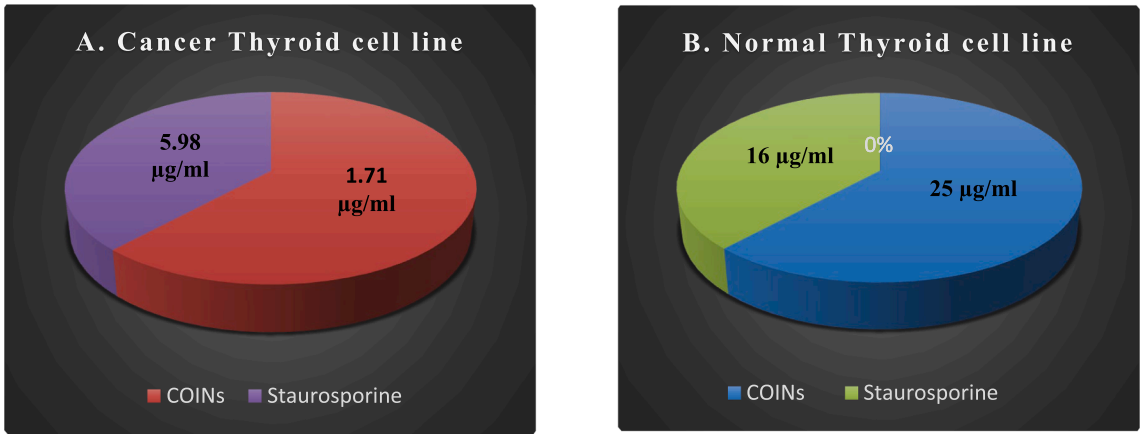

Fig. 8. IC $_{50}$ of COINs and Staurosporine against c ancer and normal thyroid cell lines.

isolates.

Till now, there has been no study on the effect of iron oxide nanoparticulates on thyroid cancer. Thyroid carcinoma is the most prevalent malignant tumor of the human endocrine system. The MTT assay was used to investigate the effects of COINs on the viability of TT cancer thyroid cell lines and N thy-ori 3–1 normal thyroid cell lines. The concentration of COINs that lowers cell viability by 50 % (IC50) was found to be 1.71 ± 0.1 µg/ml in TT cell lines. However, for N thy-ori 3–1 cell lines, IC_{50} was observed at 25.9 ± 1.6 µg/ml. Moreover, the toxicity of COINs was observed on normal cell lines at high concentrations (25.9 ± 1.6 µg/ml) compared to staurosporine (16.2 ± 0.9 µg/ml) (Table 2 and Fig. 8).

4. Discussion

Cystoseira members produce a wide range of potentially bioactive substances, including terpenoids, fatty acids, triacylglycerols, steroids, phlorotannins, and polysaccharides, which highlight the genus' importance (de Sousa et al., 2017).

The UV absorbance peak of COINs at 290 nm agreed with the absorption peaks of iron oxide nanoparticles by Das et al., 2014 and Abbas et al., 2020 (Kumar Das et al., 2014; Abbas et al., 2020). The mechanism of iron oxide nanoparticles depends on the biologically active metabolites of the Cystoseira *spp.* water extract, such as carbohydrates or sugar alcohols, which are detected by GC mass spectroscopy. Mannitol is a type of sugar alcohol, or polyol, that is produced from the reduction of carbohydrates and is in control of osmoregulation in macroalgae (Iwamoto and Shiraiwa, 2005). Similar to our results, Andrade et al., 2012 detected that *Cystoseira* species are rich sources of mannitol (Paula et al., 2013). Further, Pell and coworkers (2013) found glycerol-arsenosugar in the brown algae *Cystoseira* spp (Pell et al., 2013). It's known that sugar alcohols act as scavengers of reactive oxygen species, thereby avoiding the peroxidation of lipids and consequently destroying cells (Stoop et al., 1996). The IR and GC mass spectroscopy indicate that sugar alcohols (especially mannitol) over the surface of COINs were the cause of the synthesis and stabilization of CIONs. In this regard, Gawali et al. (2017) use D-mannitol as a coat for the stabilization of iron oxide nanoparticles, which are prepared chemically by coprecipitation (Gawali et al., 2017). This is the first work to prove the role of mannitol and other sugar alcohols in the Cystoseira spp. extract in the biosynthesis and stabilization of iron oxide nanoparticles.

For COINs Characterization Similarly, Ur Rahman et al., 2017 confirmed the atomic percentages received from EDX quantification were 48.98 % of O, 8.83 % of Fe. Also, they explained the origin of the Cl signal was Fe $(NO_3)_3{\cdot}9H_2O$ precursor and the gooseberry leaf extract used for the synthesis of nanoparticles (Rahman et al., 2017).

On the basis of MRSA resistance, similarly, Sabir et al. (2014) showed that MRSA pathogens have high susceptibility to vancomycin (100 %) and erythromycin. In addition, fifty percent of the Ciprofloxacin MRSA resistance was isolated in Indian literature (Sabir et al., 2014).

Recently, ZnO nanoparticles, CuO nanoparticles, and α-Fe2O3 have been revealed to exhibit antimicrobial potential, which comes in agreement with our study (Horst, 2009; Abbas et al., 2020). The proper explanation for why the inhibition of MRSA growth needs high concentrations of COINS may be that the outer cell wall of gram-positive bacteria contains a thick peptidoglycan coating that acts as a barrier against most inhibitory compounds and leads to the hard absorption of iron nanoparticles (Guzman et al., 2012).

Furthermore, the antibacterial efficiency of iron oxide- nanoparticles may be influenced by the reaction between ions released from nanomaterials and proteins with thiol groups (−SH) on the bacterial cell surface (Salem and IsmailMM, 2019). For the higher inhibition zones of amikacin, linezolid, vancomycin, and, in some cases, ciprofloxacin compared to the inhibition zones of COINs, we recommended in future studies the combination of antibiotics with COIN, which may have a synergistic effect to combat MRSA infection. It was reported by Abbas et al. that iron oxide nanoparticles cause morphological modifications and shape distortion in cancer cell lines (Abbas et al., 2020).

The cytotoxic effect of low doses of COINs can be explained by the charge of coating materials (as sugar alcohols), which are provided on iron oxide nanoparticles, which may change the surface charge of the nanoparticles, affecting protein absorption and subsequent biological behaviors (Feng et al., 2018). Xiao et al., for example, found that strongly positive or negatively charged micellar nanoparticles were substantially absorbed by macrophages in the liver, whereas slightly negative-charged nanoparticles had the lowest macrophage absorption and the maximum tumor uptake, which comes in agreement with our study (Xiao et al., 2011). Biological stabilizing molecules, play an essential role in determining the toxic nature of metal nanoparticles. There is also a variation in the toxic nature of nanomaterials depending on their size, reductants, and capping materials (Xiao et al., 2011). It can be concluded from the above facts that, depending on how nanomaterials are synthesized, the toxic nature of the nanomaterial will differ. Moreover, to overcome antibiotic resistance and enhance their efficacy, COINs can be combined with antibiotics. Antibiotics can be taken at a lower dose and with less toxicity when they are taken with them (Xiao et al., 2011). Future in vivo studies of COINs are highly recommended to evaluate their toxicity and therapeutic purposes against MRSA infection.

5. Conclusion

The biogenic fabrication of iron oxide nanoparticles using sugar alcohol from *Cystoseira* spp. extract is the technique presented in this

study. The high concentration of these nanoparticles was found to display antimicrobial activity against Methicillin-resistant *Staphylococcus aureus*. The thick peptidoglycan coatings on their outer cell walls act as a barrier against most inhibitory compounds and allow iron nanoparticles to be absorbed well. For that reason, the suppression of bacterial growth needs a high concentration of these nanoparticles. Furthermore, the cytotoxic effect of nanoparticles against thyroid normal cell lines and thyroid cancer cell lines in low doses could explained by the negative charge of sugar alcohols coated the nanoparticles, which affect protein absorption and subsequent biological behaviors. Future in vivo studies for the cytotoxic effect of these nanoparticles against thyroid cancer and MRSA infection are recommended.

Funding

This study wasn't supported by any fund.

CRediT authorship contribution statement

Heba S. Abbas: Writing – original draft, Methodology. **Tarek A.M. Ismaeil:** Resources. **Entesar A. Ahmed:** Supervision, Resources. **Doha H. Abou Baker:** Writing – review & editing, Methodology.

Declaration of Competing Interest

The authors declare that they have no known competing financial interests or personal relationships that could have appeared to influence the work reported in this paper.

Appendix A. Supplementary material

Supplementary data to this article can be found online at https://doi.org/10.1016/j.jksus.2024.103338.

References

Abbas, H.S., Krishnan, A., 2020. Magnetic nanosystems as a therapeutic tool to combat pathogenic fungi. Adv. Pharm. Bull. 10, 512–523.
Abbas, H.S., Krishnan, A., Kotakonda, M., 2020. The antifungal and antiovarian cancer properties of α-Fe2O3 and αFe2O3/Zno nanostructures synthesized by Spirulina platensis. IET Nanobiotechnol 14, 774–784.
Abbas, H.S., Krishnan, A., Kotakonda, M., 2020. Fabrication of Iron Oxide/Zinc Oxide Nanocomposite Using Creeper *Blepharis maderaspatensis* Extract and Their Antimicrobial Activity. Front Bioeng. Biotechnol 8, 595161.
Balouiri, M., Sadiki, M., Ibnsouda, S.K., 2016. Methods for in vitro evaluating antimicrobial activity: a review. J. Pharm. Anal. 6 (2), 71–79.
Berkov, S.H., Nikolova, M.T., Hristozova, N.I., Momekov, G.Z., Ionkova, I.I., Đilianov, D. L., 2011. GC-MS profiling of bioactive extracts from *Haberlea rhodopensis*: an endemic resurrection plant. J. Serbian ChemSoc. 76, 211–220.
Brook, I., 2009. Role of methicillin-resistant *Staphylococcus aureus* in head and neck infections. J Laryngol Otol 123, 1301–1307.
Cabizuca, C.A., Bulzico, D.A., de Almeida, M.H., Conceição, F.L., Vaisman, M., 2008. Acute thyroiditis due to septic emboli derived from infective endocarditis. Postgrad. Med. J. 84, 445–446.
Cai, W., Gao, T., Hong, H., Sun, J., 2008. Applications of gold nanoparticles in cancer nanotechnology. Nanotechnol Sci Appl 1, 17–32.
CLSI: 'Performance standards for antimicrobial disk susceptibility tests, approved standard, CLSI document M100,30th Ed. Clinical and Laboratory Standards Institute, 950 West Valley Road, Suite 2500, Wayne, Pennsylvania19087, USA., 2020.
CLSI: 'Performance standards for antimicrobial disk susceptibility tests, approved standard, CLSI document M02-A11.Clinical and Laboratory Standards Institute, 950 West Valley Road, Suite 2500, Wayne, Pennsylvania19087, USA., 2012.
de Sousa, C.B., Gangadhar, K.N., Macridachis, J., Pavao, M., Morais, T.R., Campino, L., Varela, J., Lago, J.H.G., 2017. Cystoseira algae (Fucaceae): Update on their chemical entities and biological activities. Tetrahedron Asymmetry 28 (11), 1486–1505.
El-Menshawi, B.S., Fayad, W., Mahmoud, K., El-Hallouty, S.M., 2010. El-Manawaty M (2010) Screening of natural products for therapeutic activity against solid tumors. IJEB 48, 258–264.
Elorza, J.L., Echenique-Elizonda, M., 2002. Acute suppurative thyroiditis. J Am Coll Surg 195, 729–730.
Feng, Q., Liu, Y., Huang, J., et al., 2018. Uptake, distribution, clearance, and toxicity of iron oxide nanoparticles with different sizes and coatings. Sci. Rep. 8, 2082.
Gao, Y., Chen, Y., Cao, Y., Mo, A., Peng, Q., 2021. Potentials of nanotechnology in treatment of methicillin-resistant Staphylococcus aureus. Eur J Med Chem. 213, 113056.
Gawali, S.L., Barick, B.K., Barick, K.C., Hassan, P.A., 2017. Effect of sugar alcohol on colloidal stabilization of magnetic nanoparticles for hyperthermia and drug delivery applications. J. Alloy. Compd. 725, 800–806.
Ghaemi, N., Sayedi, J., Bagheri, S., 2014. Acute suppurative thyroiditis with thyroid abscess: A case report and review of the literature. Iran J Otorhinolaryngol 26, 51–55.
Guzman, M., Dille, J., Godet, S., 2012. Synthesis and antibacterial activity of silver nanoparticles against Gram-positive and Gram-negative bacteria. NanomedNanotechnol. Biolmed 8, 37–45.
Hadied, M.O., Bardossy, A.C., Abreu-Lanfranco, O., Perri, M.P., Arshad, S., Zervos, M., Alangaden, G., 2015. Predictors of mortality in cancer patients with methicillin-resistant *Staphylococcus aureus* bloodstream infection. Open Forum Infect. Dis. 2, 838.
Horst, A.K., 2009. Antimicrobial effects of metal oxide nanoparticles', The NNIN REU Res.Accomplishments. Biol. Appl. 12–13.
Indira, T.K., Lakshmi, P.K., 2010. Magnetic nanoparticles-a review. Int. J. Pharm. Sci. Nanotechnol. 3, 1035–1042.
Iwamoto, K., Shiraiwa, Y., 2005. Salt-regulated mannitol metabolism in algae. Mar. Biotechnol. 71, 407–415.
Kaur, D.C., Chate, S.S., 2015. Study of Antibiotic Resistance Pattern in Methicillin Resistant *Staphylococcus Aureus* with Special Reference to Newer Antibiotic. J Glob Infect Dis. 7 (2), 78–84. https://doi.org/10.4103/0974-777X.157245.
Kumar Das, A., Marwal, A., Verma, R., 2014. Bio-reductive synthesis and characterization of plant protein coated magnetite nanoparticles. Nano Hybrids 7, 69–86.
Lethert, K., Bowerman, J., Pont, A., Earle, A., Garcia-Kennedy, R., 2006. Methicillin-resistant *Staphylococcus aureus* suppurative thyroiditis with thyrotoxicosis. Am. J. Med. 119, e1–e2.
Makky, E.A., AlMatar, M., Mahmood, M.H., Ting, O.W., Qi, W.Z., 2021. Evaluation of the Antioxidant and Antimicrobial Activities of Ethyl Acetate Extract of Saccharomyces cerevisiae. Food. Technol. Biotechnol. 59 (2), 127–136.
Masood, S.H., Aslam, N., 2010. In Vitro Susceptibility Test of Different Clinical Isolates against Ceftriaxone. Oman Med. J. 25 (3), 199–202. https://doi.org/10.5001/omj.2010.56.
Namvar, F., Mohamad, R., Baharara, J., Zafar-Balanejad, S., Fargahi, F., Rahman, H.S., 2013. Antioxidant, antiproliferative, and antiangiogenesis effects of polyphenol-rich seaweed (*Sargassum muticum*). BioMed. Res. Int., 604787
Paula, B.A., Mariana, B., Rui Pedro, M., Graciliana, L., Juliana, V., Teresa, M., Patrícia, V., 2013. Valuable compounds in macroalgae extracts. FoodChem 138, 1819–1828.
Pearce, E.N., Farwell, A.P., Braverman, L.E., 2003. Thyroiditis. NEJM 348, 2646–2655.
Pell, A., Kokkinis, G., Malea, P., Pergantis, S.A., Rubio, R., López-Sánchez, J.F., 2013. LC-ICP-MS analysis of arsenic compounds in dominant seaweeds from the Thermaikos Gulf (Northern Aegean Sea, Greece). Chemosphere 93 (9), 2187–2194.
Rahman, S.S.U., Qureshi, M.T., Sultana, K., Rehman, W., Khan, M.Y., Asif, M.H., Farooq, M., Sultana, N., 2017. Single step growth of iron oxide nanoparticles and their use as glucose biosensor. Results Phys. 7, 4451–4456.
Sabir, R., Alvi, S.F., Fawwad, A., Basit, A., 2014. Antibiogram of Pseudomonas aeruginosa and Methicillin-resistant Staphylococcus aureus in patients with diabetes. Pak. J. Med. Sci. 30 (4), 814–818. https://doi.org/10.12669/pjms.304.4755.
Salem, D.M.S.A., IsmailMM, A.-E., 2019. Biogenic synthesis and antimicrobial potency of iron oxide (Fe3O4) nanoparticles using algae harvested from the Mediterranean Sea Egypt. Egypt J. Aquat. Res. 43, 197–204.
Shrestha, R.T., Hennessey, J., 2000. Acute and subacute, and riedel's thyroiditis. MDText.com Inc, South Dartmouth, Mass, USA.
Stoop, J.M.H., Williamson, J., Pharr, D.M., 1996. Mannitol metabolism in plants: a method for coping with stress. Trends Plant. Sci. 5, 139–144.
Soetaert, F., Korangath, P., Serantes, D., Fiering, S., Ivkov, R., 2020. Cancer therapy with iron oxide nanoparticles: Agents of thermal and immune therapies. Advanced drug delivery reviews 163, 65–83.
Supriya, M., Shakeel, M., Santangeli, L., Ah-See, K.W., 2009. Controlling MRSA in head and neck cancer patients: what works? Otolaryngology—Head and Neck Surgery 140 (2), 224–227.
Thomas, R., Jasim, B., Mathew, J., Radhakrishnan, E.K., 2012. Extracellular synthesis of silver nanoparticles by endophytic Bordetella sp. isolated from Piper nigrum and its antibacterial activity analysis. Nano. Biomed Eng 4 (4), 183–187.
Xiao, K., Li, Y., Luo, J., Lee, J.S., Xiao, W., Gonik, A.M., Agarwal, R.G., Lam, K.S., 2011. The effect of surface charge on in vivo biodistribution of PEG-oligocholic acid based micellar nanoparticles. Biomaterials 32 (13), 3435–3446.